

# High-Density Silver Nanoparticle Film with Temperature-Controllable Interparticle Spacing for a Tunable Surface Enhanced Raman Scattering Substrate

Yu Lu, Gang L. Liu, and Luke P. Lee\*

Berkeley Sensor and Actuator Center, Department of Bioengineering,  
University of California-Berkeley, Berkeley, California 94720

Received July 4, 2004; Revised Manuscript Received November 17, 2004

## ABSTRACT

The formation of high-density silver nanoparticles and a novel method to precisely control the spacing between nanoparticles by temperature are demonstrated for a tunable surface enhanced Raman scattering substrates. The high-density nanoparticle thin film is accomplished by self-assembling through the Langmuir–Blodgett (LB) technique on a water surface and transferring the particle monolayer to a temperature-responsive polymer membrane. The temperature-responsive polymer membrane allows producing a dynamic surface enhanced Raman scattering substrate. The plasmon peak of the silver nanoparticle film red shifts up to 110 nm with increasing temperature. The high-density particle film serves as an excellent substrate for surface-enhanced Raman spectroscopy (SERS), and the scattering signal enhancement factor can be dynamically tuned by the thermally activated SERS substrate. The SERS spectra of Rhodamine 6G on a high-density silver particle film at various temperatures is characterized to demonstrate the tunable plasmon coupling between high-density nanoparticles.

Metallic nanoparticles have been the subject of extensive research in the past several years.<sup>1</sup> In particular, noble metal nanoparticles (e.g., Au and Ag) with their associated strong plasmon resonance have generated great interest in fields such as nanoscale photonics and biological sensing. The fact that particle plasmon allows direct coupling of light to resonant collective electron plasmon oscillation leads to tremendous efforts to design and fabricate optical components that can focus and manipulate light at spatial dimension far below the classical diffraction limit.<sup>2,3</sup> Silver colloidal nanoparticles are probably the most studied and best established systems, and a variety of procedures have been developed to produce monodispersed nanoparticles characterized by relatively small size variations.<sup>4</sup> A great challenge that remains is to develop effective ways to organize the nanoscale particles into functional structures and devices. Of particular interest is a general method for fabricating high-density nanoparticle films with controllable spacing on solid substrates.<sup>5–8</sup> In this report, we demonstrate a procedure for the fabrication of high-density nanoparticle film by self-assembling hydrophobic Ag nanoparticles on a water surface, transferring the particle monolayer onto a temperature-sensitive polymer substrate, and reorganizing the particles

by temperature-controlled polymer shrinkage. A very uniform, high-density nanoparticle film is generated by pushing the particles together as the polymer substrate shrinks at a certain temperature. We show that the plasmon peak red shifts when the particles get closer, in response to the temperature rise of the substrate. The high-density silver nanoparticle films can then serve as superb substrates for surface enhanced Raman spectroscopy (SERS) studies, and they have the temperature-responsive enhancement to the Raman scattering intensity of Rhodamine 6G. It has been found that the highly ordered nanoparticle film formed at a certain temperature can generate the optimal signal intensity. The thermally active high-density nanoparticle film substrate reported in this paper will have wide applications in label-free, ultra-sensitive, molecule-specific detections which utilize vibrational signatures<sup>9</sup> since it provides an ability to control precisely the spacing between nanoparticles and to find the optimized plasmon coupling distance.

Silver nanoparticles (20 nm) were prepared using oleylamine and oleic acid as the capping reagents, which can help the dissolution of reactant salt and prevent particle aggregation, oxidation and degradation, as well as render particle surface hydrophobic.<sup>10,11</sup> In a typical synthesis, 0.1 g silver nitrate ( $\text{AgNO}_3$ ) is dissolved in 1 mL oleylamine. The solution is left overnight and then diluted with 6 mL of

\* Corresponding author. E-mail: lplee@socrates.berkeley.edu.

1,2-dichlorobenzene (DCB). In a 250 mL three-neck flask, 0.3 g of 1,2-hexadecanediol in 10 mL DCB is heated to 182 °C. A 0.12 mL portion of oleic acid is then added in the hot solution. The system is kept at 182 °C for 5 min under magnetic stirring. The  $\text{AgNO}_3$ /oleylamine/DCB mixture is rapidly injected into the hot solution. A light-yellow color appears right after the injection and becomes dark brown within 1 min. The product solution is extracted after heating 5 min at 182 °C. All the synthesis is done in an argon atmosphere. To wash the sample, 3 mL of product solution is added with 5 mL of methanol, followed by 5 min centrifugation at 4000 rpm. The precipitate is redispersed in 3 mL of chloroform.

Langmuir–Blodgett (LB) is a powerful technique that can be used to assemble large-scale monolayers of hydrophobic silver nanoparticles on a water surface.<sup>12,13</sup> The technique consists of spreading a thin film of a colloidal solution of Ag nanoparticles in an organic solvent on a water surface, which has a controlled convex curvature, and allowing the solvent to evaporate. As the solvent evaporates, a monolayer of silver nanoparticles nucleates at the raised center of the water surface and grows smoothly outward. These monolayers can be transferred to a smooth substrate by bringing the substrate parallel to the water surface and lightly touching the substrate to the nanoparticle film. Multiple layers of Ag nanoparticle could be achieved by repeating this process. Figure 1 shows the structures of capping reagents (oleylamine and oleic acid), Ag nanoparticles, and the process of transforming an Ag particle film onto a polymer film. The TEM image of the Ag nanoparticles is also shown.

In a typical LB process, the film is usually pressurized to form a close-packed particle film in which particle spacing is determined by the particle diameter and the length of the surfactant molecules.<sup>14</sup> A critical factor of producing an organized, high-density particle film is that the pressure applied on the monolayer should be precisely controlled to avoid the formation of not only microscopic holes (at low pressure) but also multilayer aggregations (at high pressure). However, a perfect particle film could also be broken when the film is transferred from water surface to solid substrates. Therefore, it is not trivial to obtain a large area close-packed particle film on solid substrate by directly transferring LB film. In our process, we introduced a thermal sensitive polymer layer as the shrinkable substrate to further densify the particle monolayer, allowing the formation of high-density film of nanoparticles. Figure 2A shows the discontinuous Ag particle film obtained by directly transferring the LB monolayer to a polymer substrate without applying any pressure.

Poly (*N*-isopropylacrylamide) (PNIPAM) exhibits a low critical solution temperature (LCST) transition from 30 to 40 °C.<sup>15</sup> This response is based on the fact that in one state the network polymer chains are fully solvated and polymer has good compatibility with the solvent. As temperature goes higher than LCST, the polymer–solvent interaction is disrupted and the polymer–polymer interactions dominate, resulting in the aggregation of polymer chains. The PNIPAM thin film is prepared by photopolymerization of PNIPAM

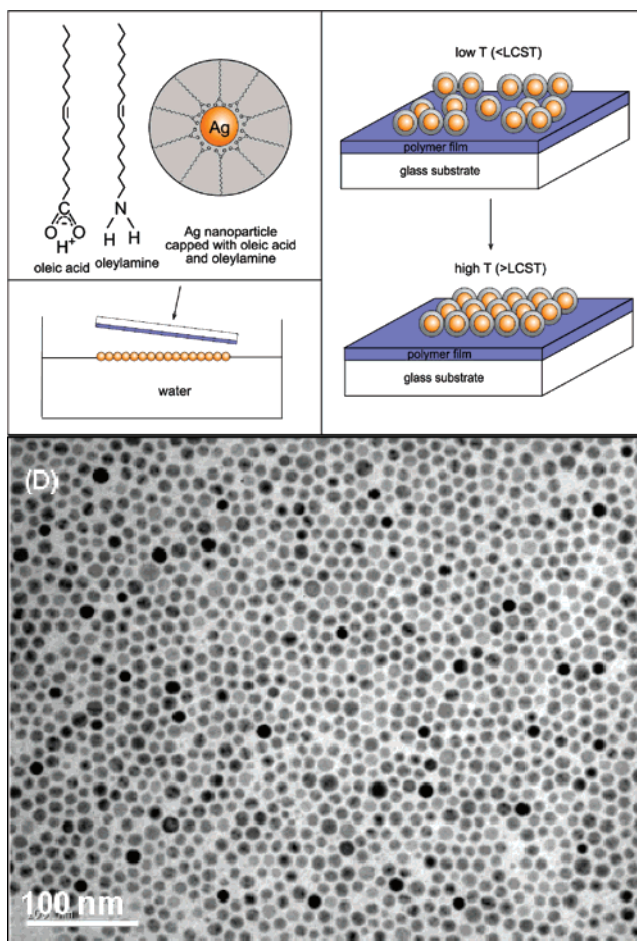


**Figure 1.** (A) Schematic structures of oleic acid and oleylamine and a silver nanoparticle capped with these surfactant molecules. (B) Schematic illustration of the experimental process of the deposition of silver nanoparticle monolayer on thermo-responsive polymer film. (C) Schematic illustration of nanoparticle monolayer on thermo-responsive polymer film. (D) A TEM image showing the size distribution of the 20 nm Ag nanoparticles.

monomers, with 2,2'-diethoxyacetophenone (DEAP) as photoinitiator and a small amount of *N,N*-methylenebisacrylamide (bis-AMD) as crosslinker. In a typical procedure, 1.6 mmol of *N*-isopropylacrylamide (NIPAM) and 30  $\mu\text{mol}$  of bis-AMD are mixed with 2 mL ultrapure water. Then 0.4  $\mu\text{mol}$  of DEAP is added into the solution as a photoinitiator. The resulting solution is dropped on a glass substrate and spread through the whole surface as it is covered with a thin glass slide to prevent oxidation. The samples were polymerized over 30 min at room temperature using attenuated UV light. After the polymer was cured, the top glass slide was removed and the polymer film in the thickness of  $\sim 100 \mu\text{m}$  could be used as the substrates to “pick up” silver nanoparticle film.

This polymer film is an ideal substrate to control nanoparticle spacing due to its ability to swell and shrink in response to temperature. As the polymer shrinks at temperatures higher than the transition temperature, most particles far away from each other can be brought together since the polymer film has about 10% or higher shrinkage. The interparticle distance became smaller and exhibits “spread out” effect in the dark-field image. Originally, there are some

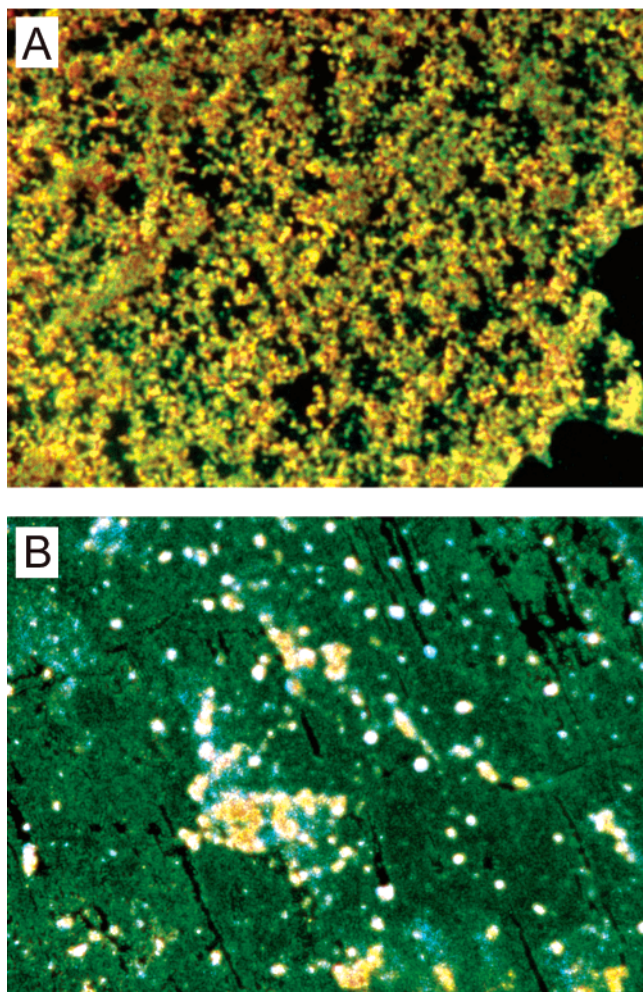


**Figure 2.** Optical dark-field microscope images of Ag nanoparticles on polymer film, poly(*N*-isopropylacrylamide). (A) The particle film obtained by directly transferring from the water surface at 20 °C. (B) The same film after the polymer substrate is heated to 40 °C.

small aggregations of silver particles that could also be brought closer by the film and thus larger particle aggregation may be present on the film at high temperature. Figure 2B shows the optical microscope image of high-density silver nanoparticle film as the result of shrinkage of the polymer substrate at 40 °C. As compared with Figure 2A, the voids and spacing are greatly reduced. Below 34 °C, water is a relatively good solvent for PNIPAM polymer and polymer chains are mostly extended, therefore, the polymer film looks transparent. In the transition regime, water becomes a poor solvent as polymer–polymer interaction becomes stronger and PNIPAM undergoes conformation changes, including both intrachain “coil-to-globule” transitions and interchain self-association. The transition leads to the volume shrinkage of the whole polymer film. As a part of reduction, the polymer surface will shrink in all directions and carry the silver particles on its surface to a closer contact. Due to the hydrophobic nature of the nanoparticle surface, the interaction between nanoparticles and the polymer substrate is so strong that the nanoparticles can reorganize to get rid of the empty spaces among broken monolayers. Though the link between particles and the film is not a chemical bond, the

mobility is caused by the interaction force between polymer molecules, and it is strong enough to bring the silver particle to move with them. The polymer film contains some water, and it takes 4 to 5 h for the film to be dry. After the film is dry in air, it cannot switch between hydrophilic and hydrophobic states.

The dependence of the absorption spectra as a function of the temperature was recorded with a UV–vis spectrometer. Figure 3A shows a typical series of UV–vis spectra at different temperatures. Figures 3B and 3C highlight the absorption spectra of the same particle film from 400 to 900 nm at 24 and 38 °C. As temperature increases from 20 to 40 °C, the plasmon peak of silver nanoparticles in the visible light region shifted from 480 to 590 nm at a temperature around 35 °C. This is mainly due to the near-field coupling between adjacent Ag particles when the Ag particles are brought together by the substrate film<sup>16</sup>, and the refractive index change of the polymer at transition temperature cannot induce such a drastic peak shift. Furthermore, an absorption peak around 800 nm appear in Figure 3C, and such near-infrared plasmon mode is also reported by others recently.<sup>17</sup> By comparing Figure 3B with 3C, the intensity of the plasmon peak in the visible light region increases more than 20 times, which can be partly attributed to the increase of the particle density in addition to the particle couplings. The phase transition of the polymer film also plays a role in the increase of absorption. The phase transition turns the polymer chain from hydrophilic to hydrophobic and breaks the interaction between the polymer chain and water molecules. The polymer film is no longer a homogeneous system, instead, it becomes a heterogeneous system composed of a hydrophobic polymer bone and small water drops. The polymer film appears semi-transparent white after phase change, thus also increases the absorption of the system, though the induced change has no spectral preference.

To estimate the relation between the average interparticle distance and temperature by analyzing the temperature-dependent absorption spectra, we simulated the absorption spectra of a monolayer cluster of 1000 (20 nm) Ag nanoparticles given various interparticle distances. We made a discrete dipole approximation to the Ag nanoparticles and numerically solved Markel’s couple dipole equations.<sup>18</sup> We used the tabulated dielectric constants of Ag at different wavelengths.<sup>19</sup> The simulation results are shown in Figure 4A. When the interparticle distance is larger than 24 nm, the absorption peak is around or below 400 nm, which is similar to the absorption peak of single Ag nanoparticle with a thin layer of coating. With the decrease of the interparticle distance, the absorption peak begins to red-shift due to the interparticle plasmon coupling. When the interparticle distance decreases to less than 12 nm, the absorption peak in the visible light region moves to the red light region, and the peaks in the near-infrared region appear. If the nanoparticles get too close to each other (<4 nm), the cluster can be considered as a bulk Ag film and the coupled dipole approximation does not apply for this case. Next we extract the absorption peak wavelengths of the Ag film at different temperatures from the measured visible light absorption

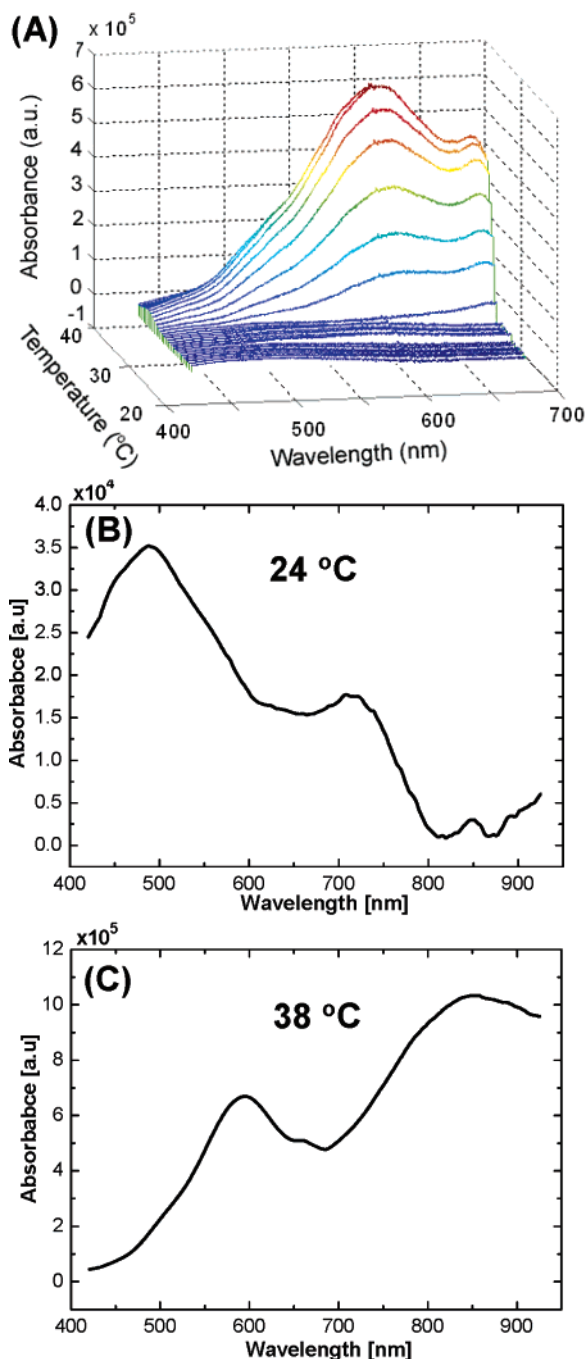


**Figure 3.** (A) UV–visible absorption spectra of a monolayer of silver nanoparticles on thermoresponsive polymer film at various temperatures. (B) and (C) highlight the absorption spectra of the same particle film from 400 to 900 nm at 24 and 38 °C, respectively. As the temperature increases from  $\sim 20$  to above 34 °C, the absorbance peak in the visible light region shifts from 480 to 590 nm and the intensity increases for more than 20 times. An absorption peak around 800 nm appears when the temperature is above 34 °C.

spectra (Figure 3A) and plot them in Figure 4B as a function of temperature. The interparticle distances at different temperature regions are estimated according to our simulation results and denoted in Figure 4B.

The high-density particle film is expected to have high local electromagnetic (EM) field enhancement and can be served as SERS substrates for molecular sensing with high

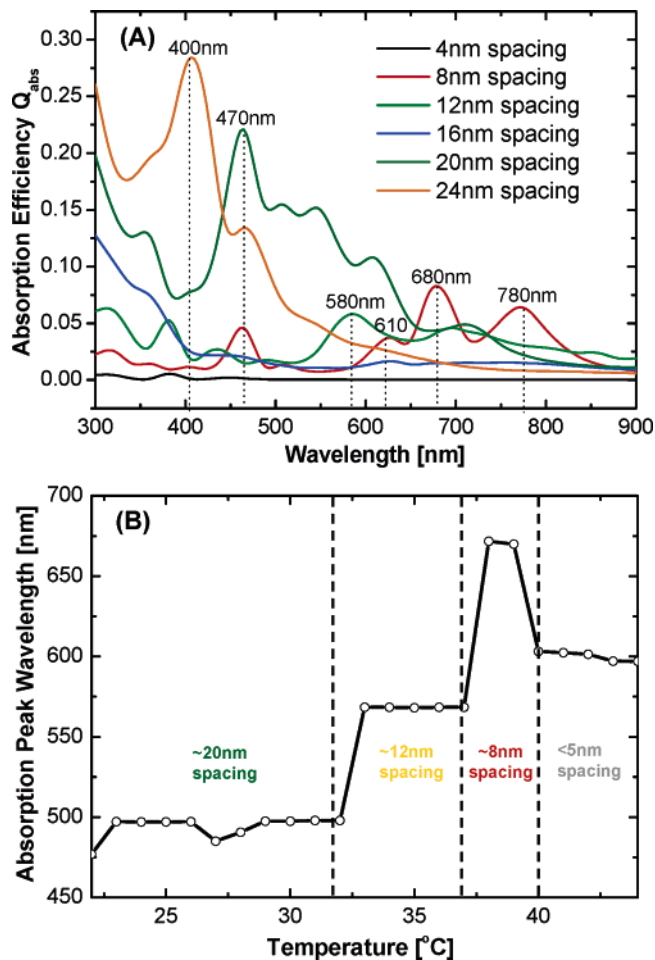


**Figure 4.** (A) Simulated absorption spectra of Ag nanoparticle clusters with different interparticle distances. (B) Absorption peak wavelength vs temperature. The interparticle distances in different temperature regions are estimated according to the simulation results.

sensitivity and specificity. The Ag nanoparticles are “floating” on the surface of the temperature-sensitive polymer layer, not embedded in the layer, so most of the Raman signal should come from the molecules adsorbed on the surface of Ag nanoparticles. Figure 5 shows a set of SERS spectra of  $10^{-5}$  M Rhodamine 6G (R6G) molecules adsorbed on a high-density Ag particle film (785 nm, 40 mV) at various temperatures. The observed Raman bands that are assigned to R6G include  $\nu(\text{C-H})$  out-of-plane bend mode at  $774\text{ cm}^{-1}$ ,  $\nu(\text{C-H})$  in-plane bend mode at  $1129\text{ cm}^{-1}$ ,  $\nu(\text{C-C})$  stretching mode at  $1363\text{ cm}^{-1}$ ,  $1509\text{ cm}^{-1}$ ,  $1650\text{ cm}^{-1}$ .<sup>20</sup> The coated oleic acid and oleylamine layer is only 1–2 nm thick, and their Raman scattering cross-sections are smaller than R6G molecules, so their Raman peaks are not as prominent as those of adsorbed R6G molecules that are still within the range of scattering near-field of Ag nanoparticles. The peaks such as  $1020$  and  $1181\text{ cm}^{-1}$  are assigned to the coated molecules. A minor background signal from the polymer and glass substrate has been subtracted in the presented figures. The intensity of the R6G Raman signal dramatically increased when the temperature goes higher than the LCST. This is due to coherent capacity coupling between adjacent particles in the high-density particle film. Calculation of

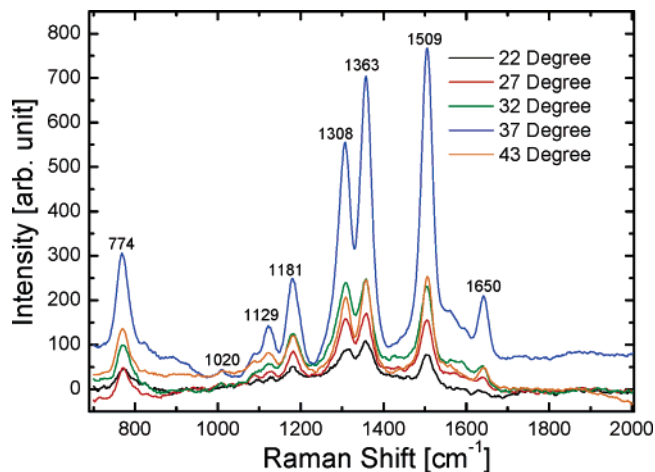


**Figure 5.** SERS spectra of Rhodamine 6G (R6G) on Ag nanoparticle film at different temperatures. The R6G concentration is  $10^{-5}$  M. The spectra are recorded using a Raman spectrophotometer (785 nm 40 mW laser excitation) and the integration time is 5 s.

particle aggregation shows that the coupling between particles is quite short-ranged.<sup>21</sup> The electromagnetic field in the particle junctions is not a simple coherent sum of the fields from each individual particle. Instead, as the particles approach each other, there is a dramatic enhancement factor increase of more than 10 times and even 100 times for certain bands (i.e.,  $1650\text{ cm}^{-1}$ ). The maximal SERS enhancement is achieved around  $37\text{ }^{\circ}\text{C}$ , at which temperature the interparticle distance makes the plasmon resonance peak of the nanoparticle cluster closer to the laser excitation wavelength. This result has good correlation with our estimation on the interparticle distance at different temperatures. Additionally, the area of active SERS substrate is increased by bringing the nanoparticle closer and minimizing the voids on the Ag film since the SERS effect is sensitive to the defect on the Ag film. When the temperature is lower than the transition temperature, the interparticle distance is larger than 12 nm and the plasmon peaks are in the blue and green light region; conversely when the temperature rises and becomes higher than the transition temperature, the interparticle distance is shorter than 12 nm which, makes the plasmon peak red shift to the far red and near-infrared light region. The observed temperature-dependent SERS spectra can be well correlated to the factors described above since a 785 nm laser excitation is used.

In conclusion, hydrophobic nanoparticles—Ag particles capped with oleic acid and oleylamine have been fabricated and used as the building components for LB technique. The as-obtained Ag nanoparticles on water surface are transferred onto a thermoresponse polymer surface. As temperature increases, the polymer undergoes a phase transition and the polymer film shrinks in all direction. The Ag particles are pushed closer by the polymer film and the particle spacing can be tuned by adjusting temperature. Highly ordered high-density particle film can be obtained by heating the film to temperature above the polymer's LCST. We have studied the optical response of the Ag nanoparticles on thermo-

response polymer film as a function of temperature dependence. The Raman spectra of R6G molecules on the Ag nanoparticles are also investigated. Raman enhancement of this tunable SERS substrate shows temperature dependence and optimal temperature and interparticle distance exist for given laser excitation line. Although comparable sensitivity has been reported, the use of our particle film as SERS substrates has the advantage of tunability. First, high-density particle film can be easily obtained. Our method can use discontinuous or broken particle film as the starting materials, and change them into dense particle film. Second, the spacing between nanoparticles can be controlled by adjusting temperature for tunable SERS substrates for optimal signal amplifications. The particle distance can be optimized to approach strongest coupling between adjacent particles and match the plasmon resonance wavelength to the laser excitation wavelength. Hence, our high-density particle film and an ability to control precisely the spacing between nanoparticles by temperature can have significant applications in label-free biomolecular detections, environmental monitoring, and biological warfare agents sensing.

**Acknowledgment.** This research was supported by grants to Y.L. from Samsung Research Fund and Nanophotonic Bioscience Fund, G.L. from Intel Research Fund, and L.P.L. from NSF Career Award.

## References

- (1) Goia, D. V.; Matijevec, E. *New J. Chem.* **1998**, 1203.
- (2) Bohren, C. F.; Huffman, D. R. *Adsorption and Scattering of Light by Small Particles*; Wiley: New York, 1983.
- (3) Charney, C.; Lee, A.; Man, S.-Q.; Moran, C. E.; Radloff, C.; Bradley, K.; Halas, N. J. *J. Phys. Chem. B* **2003**, *107*, 7327.
- (4) Xia, Y.; Sun, Y. *Anal. Chem.* **2002**, *74*, 5297.
- (5) Kim, F.; Kwan, S.; Arkana, J.; Yang, P. *J. Am. Chem. Soc.* **2001**, *123*, 4386.
- (6) Messer, B.; Song, J. H.; Yang, P. *J. Am. Chem. Soc.* **2000**, *122*, 10232.
- (7) Huang, Y.; Duan, X. F.; Wei, Q.; Lieber, C. M. *Science* **2001**, *291*, 630.
- (8) Melosh, N. A.; Boukai, A.; Diana, F.; Gerardot, B.; Badolato, A.; Petroff, P. M.; Heath, J. R. *Science* **2003**, *300*, 112.
- (9) Tao, A.; Kim, F.; Hess, C.; Goldberger, J.; He, R.; Sun, Y.; Xia, Y.; Yang, P. *Nano Lett.* **2003**, *3*, 1229.
- (10) Quaroni, L.; Chumanov, G. *J. Am. Chem. Soc.* **1999**, *121*, 10642.
- (11) Nagasawa, H.; Maruyama, M.; Komatsu, T.; Isoda, S.; Kobayashi, T. *Phys. Status Solidi A* **2002**, *191*, 67.
- (12) Kwan, S.; Kim, F.; Arkana, J.; Yang, P. *Chem. Commun.* **2001**, *5*, 447.
- (13) Chung, S. W.; Markovich, G.; Heath, J. R. *J. Phys. Chem. B* **1998**, *102*, 6685.
- (14) Heath, J. R.; Knobler, C. M.; Leff, D. V. *J. Phys. Chem. B* **1997**, *101*, 189.
- (15) Serpe, M. J.; Jones, C. D.; Lyon, L. A. *Langmuir* **2003**, *19*, 8759.
- (16) Krenn, J. R.; Dereux, A.; Weeber, J. C.; Bourillot, E.; Lacroute, Y.; Goudonnet, J. P.; Schider, G.; Gotschy, W.; Leitner, A.; Aussenneg, F. R.; Giarad, C. *Phys. Rev. Lett.* **1999**, *82*, 2590.
- (17) Mertens, H.; Verhoeven, J.; Polman, A.; Tichelaar, F. D. *Appl. Phys. Lett.* **2004**, *85*, 1317.
- (18) Markel, V. A. *J. Mod. Opt.* **1993**, *40*, 2281.
- (19) Johnson, P. B.; Christy, R. W. *Phys. Rev. B* **1972**, *6*, 4370.
- (20) Hildebrandt, P.; Stockburger, M. *J. Phys. Chem.* **1984**, *88*, 5935.
- (21) Jiang, J.; Bosnick, K.; Maillard, M.; Brus, L. *J. Phys. Chem. B* **2003**, *107*, 9964.

NL048965U